Published by AIT
the Italian Society of Remote Sensing

Assessing vegetation variability and trends in north-eastern Brazil using AVHRR and MODIS NDVI time series

Anne Schucknecht[1*], Stefan Erasmi[2], Irmgard Niemeyer[3] and Jörg Matschullat[1]

[1]Interdisciplinary Environmental Research Centre, TU Bergakademie Freiberg,
Brennhausgasse 14, 09599 Freiberg, Germany
[2]Institute of Geography, Georg-August University Göttingen,
Goldschmidtstraße 5, 37077 Göttingen, Germany
[3]Institute of Energy and Climate Research, IEK-6,
Forschungszentrum Jülich GmbH, 52425 Jülich, Germany
*Corresponding author, e-mail address: anne.schucknecht@ioez.tu-freiberg.de

Abstract
Desertification is a challenge in north-eastern Brazil (NEB) that needs to be understood to develop sustainable land-use strategies. This study analyses regional vegetation dynamics in NEB and the compatibility of two NDVI data sets to support future desertification assessment studies in the semi-arid Caatinga biome. Vegetation variability and trends in NEB are analysed for 1982-2006, based on monthly AVHRR (GIMMS) NDVI data. The GIMMS data are compared with MODIS NDVI for the overlapping period 2001-2006. Existing statistical methods are applied and existing NDVI analyses in NEB expanded in respect to vegetation trend analysis and data set comparison.

Keywords: Normalized Difference Vegetation Index, Cerrado, Atlantic Forest, time series decomposition, BFAST, precipitation.

Introduction
Desertification, defined as "land degradation in arid, semiarid, and dry sub-humid areas resulting from various factors" [UNCED, 1992], is a serious challenge in north-eastern Brazil (NEB). Large areas are susceptible to or already affected by desertification processes [MMA, 2007]. Knowledge about desertification processes and underlying causes is needed to develop sustainable land-use strategies for the region. This issue motivates studying vegetation dynamics in NEB, as vegetation variability and trends represent important aspects of the complex desertification concern. Long time-series of satellite data are suitable to assess vegetation dynamics on a regional scale.
Satellite remote sensing data are an established source for monitoring ecosystem dynamics

[Coppin et al., 2004]. Vegetation indices (VIs) have demonstrated their usefulness in monitoring light-dependent physiological processes such as photosynthesis, as they are almost linearly related to the fraction of photosynthetically active radiation (fPAR) absorbed by a plant canopy [Glenn et al., 2008]. Normalized Difference Vegetation Index (NDVI) data, calculated as a nonlinear combination of red and near infrared (NIR) reflectances (NIR - RED)/(NIR + RED), from the National Oceanic and Atmospheric Administration (NOAA) Advanced Very High Resolution Radiometer (AVHRR) with global coverage and 8 km resolution, have been applied for numerous regional to global vegetation studies since they became available in 1981 [Fensholt et al., 2009]. More recent global NDVI data sets provide a higher spatial resolution and are considered an improvement compared to AVHRR [Fensholt et al., 2009]. This includes data, e.g., from Terra Moderate Resolution Imaging Spectroradiometer (MODIS; 250 m to 1 km) [e.g., Huete et al., 2002; Justice et al., 2002; Tucker and Yager, 2011] and Système Pour l'Observation de la Terre (SPOT) VEGETATION mission (1 km) [e.g., Durpaire et al., 1995]. A combination of the AVHRR NDVI time series with those NDVI time series is desirable to combine the advantages of AVHRR data (longest time span) with the higher spatial resolution of the more recent data sets. Some studies were undertaken to evaluate the general compatibility of AVHRR data and MODIS NDVI showing that MODIS in general has higher NDVI values than AVHRR [Fensholt and Sandholt, 2005; Brown et al., 2006]. Fensholt et al. [2009] found that annual average value trend analysis of AVHRR NDVI from Global Inventory Modelling and Mapping Studies (GIMMS) data is consistent with Terra MODIS NDVI for the semi-arid Sahelian zone, whereas more humid areas show higher discrepancies.

Different studies have addressed vegetation characteristics in NEB by the application of NDVI data. Large-scale studies of entire NEB, based on GIMMS NDVI time series [Barbosa et al., 2006; Erasmi et al., 2009], showed a high spatial and temporal (intra- and inter-annual) vegetation variability. Both studies indicated that the seasonal NDVI oscillation is related to the seasonal distribution of precipitation (wet and dry periods). The NDVI follows the rainfall patterns with a displacement of one to two months [Erasmi et al., 2009]. The highest temporal variability of NDVI as well as the highest correlation of NDVI and precipitation is found for the semi-arid region of the Caatinga [Erasmi et al., 2009]. A similar behaviour, i.e. a decrease of the ecosystem´s sensitivity to annual precipitation with increasing mean annual precipitation, was observed for African savannas [Chamaillé-Jammes and Fritz, 2009] and several American biomes [Huxman et al., 2004].

Studies on vegetation changes (including land degradation issues) in NEB were conducted on different spatial scales. Local to small regional scale studies (< 4000 km^2) applied, e.g., floristic and phytosociological inventories [da Costa et al., 2009], and SPOT images in combination with field work [Costa Filho et al., 2008], Landsat Thematic Mapper (TM) and Enhanced Thematic Mapper (ETM) imagery [Petta et al., 2005; Almeida-Filho and Carvalho, 2010]. Barbosa et al. [2006] analysed vegetation trends for NEB by calculating standardized anomalies of monthly NDVI values (regional mean values of all pixels within NEB). The authors identified a consistent upward trend in vegetation greenness between 1984 and 1990 and a reversed trend in the subsequent period from 1991 to 1998. De Jong et al. [2012] demonstrated the importance of accounting for trend changes during the analysis of long-term vegetation time series.

In this study, we analysed a 25-year monthly time series (1982-2006) of GIMMS AVHRR

NDVI data to characterize vegetation dynamics. We calculated the means and coefficients of variation of monthly NDVI values as well as different trend estimators on a pixel basis (spatial resolution 8 km) and as regional mean values for NEB. Trends were also analysed for monthly precipitation data to assess possible relations to vegetation trends. The temporal NDVI and precipitation development of four selected regions of interest (ROIs) was studied by applying time series decomposition. Monthly NDVI time series of GIMMS AVHRR and MODIS vegetation product (MOD13A3) from 2001-2006 were used to evaluate the compatibility of both data sets (on a spatial resolution of 8 km). Monthly mean values, coefficient of variation, and different trend estimators were calculated and compared. Additionally, a linear regression was performed to analyse the correlation coefficient and the determination coefficient. The study applies existing statistical methods to deepen existing NDVI analyses for entire NEB in respect of the vegetation trend analysis and the data set comparison.

Study area

North-eastern Brazil (NEB) is located between ~1° to 19° S and ~34° to 49° W and covers an area of ~1.6 million km^2, showing a large natural diversity with respect to, e.g., climate, vegetation, geology, and soil [Matschullat et al., 2012]. NEB is under tropical influence, characterized by a hot climate with average temperatures above 18°C in all months [IBGE, 2002]. Hydrological settings range in extremes from semi-desert environments of the "Sertão" in the central eastern part (precipitation < 500 mm year $^{-1}$, 9-11 dry months) to rainwater-rich coastal environments along the Atlantic ocean (~2000 mm year $^{-1}$, no dry months) [IBGE, 2002; CPRM, 2009]. Precipitation shows a seasonal cycle generated by the shift of the Inter-tropical Convergence Zone [Nimer, 1989]. Four continental biomes cover NEB [IBGE, 2004a] (Fig. 1): 1) The Atlantic Forest (Mata Atlântica) stretches along the eastern coast of Brazil - yet only remains of the original Atlantic forest exist today [Morellato and Haddad, 2000]. 2) The Caatinga - a xeric scrubland and open thorn forest - in the central part of NEB covers substantial parts of NEB. 3) The Cerrado - a tropical savanna - is more densely covered than the Caatinga and stretches westward of the Caatinga. 4) The north-western part of NEB belongs to the Amazon Rainforest, yet large areas of the original vegetation have been changed to secondary vegetation and agricultural areas [IBGE, 2004b]. Generally, the natural vegetation in NEB has been seriously altered by land use changes over the last few decades [Simielli, 2007] and large areas of NEB now show anthropogenically influenced vegetation types such as secondary vegetation or agriculture (Fig. 6D) [IBGE, 2002].

Data sets and methods

Satellite based vegetation indices data

We used the GIMMS NDVI data product [Tucker et al., 2004], available from the Global Land Cover Facility of the University of Maryland (www.landcover.org) to analyse the long-term (25 years) vegetation variability and vegetation trends in NEB. The NDVI data set was derived from imagery, obtained from the AVHRR instrument on board the NOAA satellite series 7, 9, 11, 14, 16, and 17. The data was corrected for viewing geometry, calibration, volcanic aerosols, and other effects not related to vegetation change [Pinzon et al., 2005; Tucker et al., 2005]. The original GIMMS data set provides bi-monthly maximum value composites of NDVI from July 1981 to December 2006 with a spatial resolution of 8 km.

The global data set was cut to the extent of NEB and the bi-monthly data were aggregated to monthly composites by applying the arithmetic mean of each month. A linear temporal interpolation was applied to replace "no data" entries. We used full year data, and analysed a set of 300 image channels ranging from January 1982 to December 2006.
NDVI time series (2001-2006) from the MODIS on board the Earth Observing System Terra platform were used for the comparison of the GIMMS data with a higher spatial resolution data set. We analysed the NDVI time series of the MODIS vegetation indices product MOD13A3 with a temporal resolution of one month and a spatial resolution of 1 km [NASA Land Processes Distribute Active Archive Center, 2010]. The MODIS NDVI products are "computed from atmospherically corrected bi-directional surface reflectances that have been masked for water, clouds, heavy aerosols, and cloud shadows" [NASA Land Processes Distribute Active Archive Center, 2012]. For every time step, we mosaicked the four tiles covering NEB and cut the resulting images to the extent of NEB. "No data" entries were replaced by applying a linear temporal interpolation.

Precipitation data
Gridded monthly precipitation sums from 1982-2006 with a spatial resolution of 0.5° were taken from the Land-surface Full Data Product Version 5 [Rudolf and Schneider, 2005; Rudolf et al., 2010], provided by the Global Precipitation Climatology Centre (GPCC; http://gpcc.dwd.de). The GPCC data set represents a Full Data Reanalysis product, based on global weather observations [Schneider et al., 2011]. The data set was cut to the extent of NEB and analysed for long-term trends and trend breaks (see below).

Statistical analysis
Basic statistical parameters like mean, standard deviation (SD), and coefficient of variation (CV) were calculated on a monthly basis for every pixel over the entire study period (1982-2006) for the GIMMS data. A binary mask of the study area (excluding pixels with negative monthly mean values) was applied to calculate regional mean values and to exclude pixels with fill values (e.g., pixels of large water-bodies such as Atlantic ocean pixels) and other negative (non-vegetation) pixels (occurring at the transition of larger water bodies and land) from the calculation. These regional mean values were calculated for monthly mean NDVI and for certain trend parameters (see below).

Long-term trend calculation
Time series can be decomposed in a trend, seasonal, and remainder component. The applied long-term trend estimators are intended to be used with de-seasoned data [Eastman, 2009]. Standardised anomalies (Z) of the monthly time series were calculated to remove the seasonality from the original time series:

$$Z = (x - \mu) / \sigma \quad [1]$$

where x is the data value of the respective month, μ is the monthly mean value (i.e., January mean, February mean, …), and σ is the monthly standard deviation. The standardised anomaly time series was just applied for the long-term trend calculation, not for the general

statistics and the trend break analysis.

Three types of inter-annual trend analysis and one trend significance test were performed for the study period 1982-2006 on a pixel basis: linear trend (OLS), median trend (Theil-Sen), monotonic trend (Mann-Kendall), and Mann-Kendall significance.

The calculated linear trend is based on the slope coefficient of an ordinary least square regression (OLS slope) between the values of each pixel over time and a perfectly linear series. The result gives the rate of change per time step (e.g., for monthly data: rate of change per month) [Eastman, 2009].

The median trend after Theil-Sen is a robust non-parametric trend operator, recommended for the assessment of the rate of change for short or noisy series. The result (TS slope) is often identical to the OLS output for long time series. The Theil-Sen operator is determined by calculating the slope between every pair-wise combination and then assessing the median. The breakdown bound for the median trend is about 29%, meaning the trends expressed in the image must have persisted for >29% of the length of the series (in time steps) [Gilbert, 1987; Eastman, 2009].

The monotonic Mann-Kendall trend represents a non-linear trend indicator measuring the degree to which a trend is consistently decreasing or increasing. The Mann-Kendall statistic (MK τ) is calculated by evaluating all pair-wise combinations of values over time at each pixel and counting the number decreasing or increasing with time. The Mann-Kendall statistic is the relative frequency of decreases minus the relative frequency of increases and ranges from -1 to 1.

The Mann-Kendall significance (MK Z) expresses the significance of a Mann-Kendall trend, but is also used as a trend test for the Theil-Sen median slope operator. The resulting significance image shows Z-scores, expressing certain levels of significance (α): $Z = \pm 2.576$ refers to $\alpha = 0.01$, $Z = \pm 1.960$ refers to $\alpha = 0.05$, and $Z = \pm 1.645$ refers to $\alpha = 0.1$ [Gilbert, 1987; Eastman, 2009]. For example, if a certain region expresses a MK Z of +2.576, it means that the calculated Mann-Kendall trend is positive and significant at a significance level α of 0.01. In the following, areas with a MK Z between -1.960 and +1.960 (corresponds to $\alpha \geq 0.05$) are referred to no trend areas.

Calculation of trend breaks

The long-term trend calculations just show the overall trend of the entire study period and give no hints, whether different sub-periods with no or opposite trends exist within the study period. Therefore, we additionally performed a trend break or trend change analysis. A trend break in a time series indicates that the trends change between positive and negative within the analysis period [de Jong et al., 2012].

Four regions of interest (ROIs) were selected to show the temporal NDVI variation and development for small areas (location of ROI in Fig. 1). The squared ROIs with a spatial extent of 7 x 7 pixels (one pixel ~ 8 km x 8 km) were selected on the basis of the NDVI analysis results (mean, trend calculation) to meet the following requirements: I) Notable long-term trend and II) relative homogeneous mean monthly NDVI values. A summary of this parameters and the associated vegetation type [after IBGE, 2004b] for every ROI is given in Table 1. The mean of all pixels within a certain ROI was extracted for each time step to create a NDVI time series of a ROI. We applied the Breaks For Additive Seasonal and Trend (BFAST) method developed by Verbesselt et al. [2010a, b] to detect changes in the seasonal and trend component of the ROI times series. BFAST combines time series decomposition into trend, seasonal, and remainder

component, and methods for change detection within time series.

Table 1 - Vegetation characteristics of the ROIs used for the BFAST analysis. Mean NDVI, CV, and MK *Z* refer to the GIMMS NDVI time series (1982-2006); given is the mean, min, and max of all pixels within the ROI. Simplified vegetation types according to Fig. 6D and after IBGE [2002]: Sav = savanna, Ste = steppe-like savanna, Ant = anthropogenically influenced regions (secondary vegetation or agriculture).

ROI	Mean NDVI			CV [%] of NDVI			MK *Z*			Vegetation type
	min	max	mean	min	max	mean	min	max	mean	
#1	0.43	0.54	0.49	12.5	22.7	18.2	3.71	9.40	6.59	Sav
#2	0.51	0.64	0.56	14.2	29.2	21.4	-6.89	1.16	-3.01	almost all Ant, very few Sav
#3	0.44	0.62	0.50	18.8	36.3	31.4	0.90	5.76	3.62	about 2/3 Ste, 1/3 Ant
#4	0.37	0.57	0.45	25.5	43.1	36.4	-7.06	1.47	-3.00	mainly Ant, few Ste

The approach is available in the BFAST package for R [R Development Core Team, 2012] from CRAN (http://cran.r-project.org/web/packages/bfast/index.html). A detailed description of the motivation and algorithms is given in the afore-mentioned publications. BFAST can be applied to seasonal and non-seasonal time series, requiring only the parameterisation of the minimal segment size between potentially detected breaks (h). In our analysis we set h to 0.15 in line with Verbesselt et al. [2010a] and de Jong et al. [2012]. Additionally, the BFAST method was applied to the monthly precipitation data of the same four ROIs as for the NDVI data to compare the trend behaviour of both variables.

Comparison of NDVI data sets

The prerequisite condition to combine NDVI data from different data sets (acquired at different time periods) is that they show similar NDVI signals over time. To test this assumption for the GIMMS and MODIS data sets, we evaluated monthly NDVI values for the overlapping period of 2001-2006. Therefore, the MOD13A3 data was re-sampled to the spatial resolution of the GIMMS data set (8 km) by applying a bilinear method. We calculated the monthly mean, the coefficient of variation, and different trend estimators (see section "Long-term trend calculation") of both data sets for the period 2001-2006 and compared the resulting images of both data sets as well as a difference image for the monthly mean. Additionally, we performed a linear regression between monthly NDVI data of GIMMS and MODIS (with MODIS NDVI as the independent variable), and evaluated the coefficient of correlation (r) and the coefficient of determination (r^2).

In terms of a user-based analysis, we want to examine, how good both datasets correlate and if certain natural factors influence the compatibility. Therefore, we set the results of the data set comparison in relation to vegetation characteristics like mean NDVI and CV, and cloud cover (see below). It is not the aim of this work to explain the technical reasons (e.g., effects of bidirectional reflectance distribution function, spectral response function, physical sensor settings) for differences in both data sets.

Clouds can obstruct the Earth´s surface and introduce noise to the data. The use of composite

data is one possibility to deal with the effects introduced by clouds, but may not always work in regions with persistent cloud cover. We calculated the monthly mean of the quality information (pixel reliability) of the MODIS data and compared the resulting image with the pattern in the correlation image to evaluate the potential influence of clouds (image quality in general) on the correlation analysis. The pixel reliability of the MOD13A3 data includes the following classes: 0 refers to good data, 1 to marginal data, 2 to snow/ice, and 3 to cloudy data.
General image pre-processing and calculation of basic statistics were done with ENVI 4.7. Filtering, de-seasonalization, linear modelling, and trend calculations were performed with IDRISI 16.05 Taiga Edition. The maps were created with ESRI® ArcMap™ 9.3.1.

Results and discussion

Vegetation variability and vegetation trends in NEB

The spatial and temporal variability of the NDVI in NEB was studied in detail by Barbosa et al. [2006] for the period 1982-2001 and by Erasmi et al. [2009] for the period 1982-2006. Therefore, we briefly present an overview on the vegetation variability to support the following trend analysis. Mean NDVI (Fig. 1A) and coefficient of variation (CV; Fig. 1B) indicate high vegetation variability in space and time for NEB. The major biomes of the study area - Caatinga, Cerrado, and Atlantic Forest - and partly even certain vegetation types (Fig. 6D) are reflected by mean NDVI and CV. The Amazon Rainforest biome in the extreme northwest is not clearly distinguishable from the Cerrado. The Caatinga region represents the lowest mean NDVI and the highest temporal variation as a consequence of the relatively low annual precipitation and the more extended dry periods. NEB is characterized by a mean NDVI of 0.52 for the period 1982-2006.
The applied trend estimators (OLS slope, TS slope, MK τ) reveal similar trend patterns and a similar amount of areas with negative/positive trend estimator values (Tab. 2) for NEB. Therefore, only the Mann-Kendall significance with an indication of trend direction and trend significance is shown in the figure (Fig. 1C). Negative (positive) trends of red/near-infrared vegetation indices are referred as browning (greening) [de Jong et al., 2012], as these indices indicate chlorophyll abundance and are therefore related to vegetation amount and photosynthetic capacity [Myneni et al., 1995].

Table 2 - Trend analysis results for entire NEB for monthly NDVI time series of GIMMS (1982-2006). OSL = ordinary least square, TS = Theil-Sen, MK = Mann-Kendall.

Trend estimator/ significance	Mean	Area with negative values [%]	Area with positive values [%]	Area with significant negative trend [%]	Area with significant positive trend [%]
OSL slope	0.0006	33.18	66.82	/	/
TS slope	0.0005	36.86	63.14	/	/
MK τ	0.0299	36.36	63.64	/	/
MK Z	0.7716	36.37	63.63	10.44	27.62

About 10% of NEB are affected by significantly negative NDVI trends ($\alpha = 0.05$) and about 28% by positive trends over the 1982-2006 period. Northwestern NEB is dominated by a greening

trend. Other adjacent areas with a greening trend are for example located in the southwest and in central NEB (southwest of Ceará). Larger areas with a browning trend are among others located in the southwest of Rio Grande do Norte and close to the coast in southern Sergipe and northeastern Bahia. The overall trend pattern looks quite patchy over NEB (Fig. 1C).

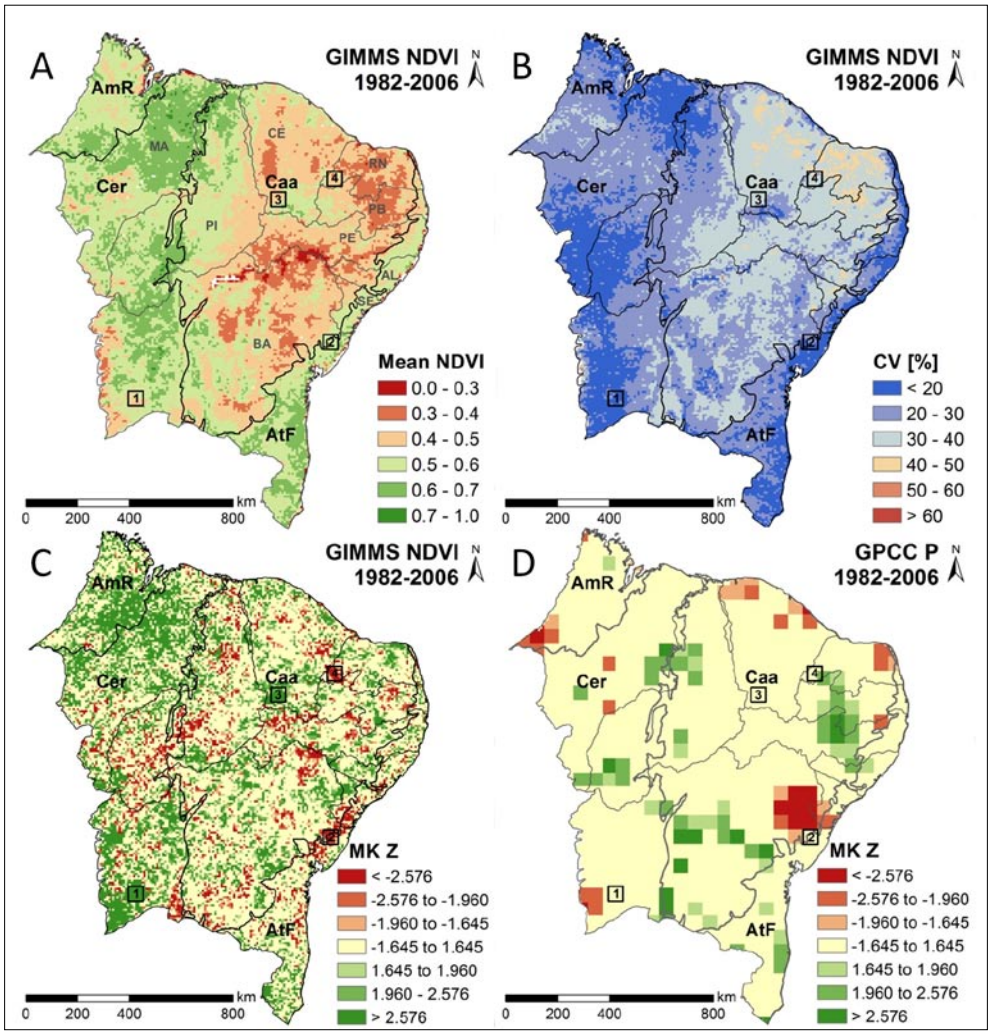

Figure 1 - Monthly NDVI values from GIMMS and monthly precipitation sums for 1982-2006. A) Monthly mean NDVI; B) coefficient of variation of monthly NDVI; C) Mann-Kendall significance of de-seasoned NDVI time series (standardised anomalies): $Z = \pm 2.576$ refers to $\alpha = 0.01$, $Z = \pm 1.960$ refers to $\alpha = 0.05$, $Z = \pm 1.645$ refers to $\alpha = 0.1$; D) Mann-Kendall significance of de-seasoned precipitation time series. Black lines indicate biome borders after IBGE [2004a]: AmR = Amazon Rainforest; Cer = Cerrado; Caa = Caatinga; AtF = Atlantic Forest. Grey lines represent state borders: AL = Alagoas; BA = Bahia; CE = Ceará; MA = Maranhão; PB = Paraíba; PE = Pernambuco; PI = Piauí; RN = Rio Grande do Norte; SE = Sergipe.

De Jong et al. [2012] studied global greening and browning trends based on GIMMS NDVI in the period 1982-2008 and highlighted the importance to consider trend changes (break points; change between greening and browning) in long-term analysis. NDVI trend changes are especially relevant for NEB, as NEB was one of the regions with the highest amount of breakpoints (mainly two to four), whereby around 60% of the global land area were affected by no or just one trend change [de Jong et al., 2012]. The time series analysis of ROIs in this study illustrates exemplarily different trend behaviour and trend changes in NEB (Fig. 2).

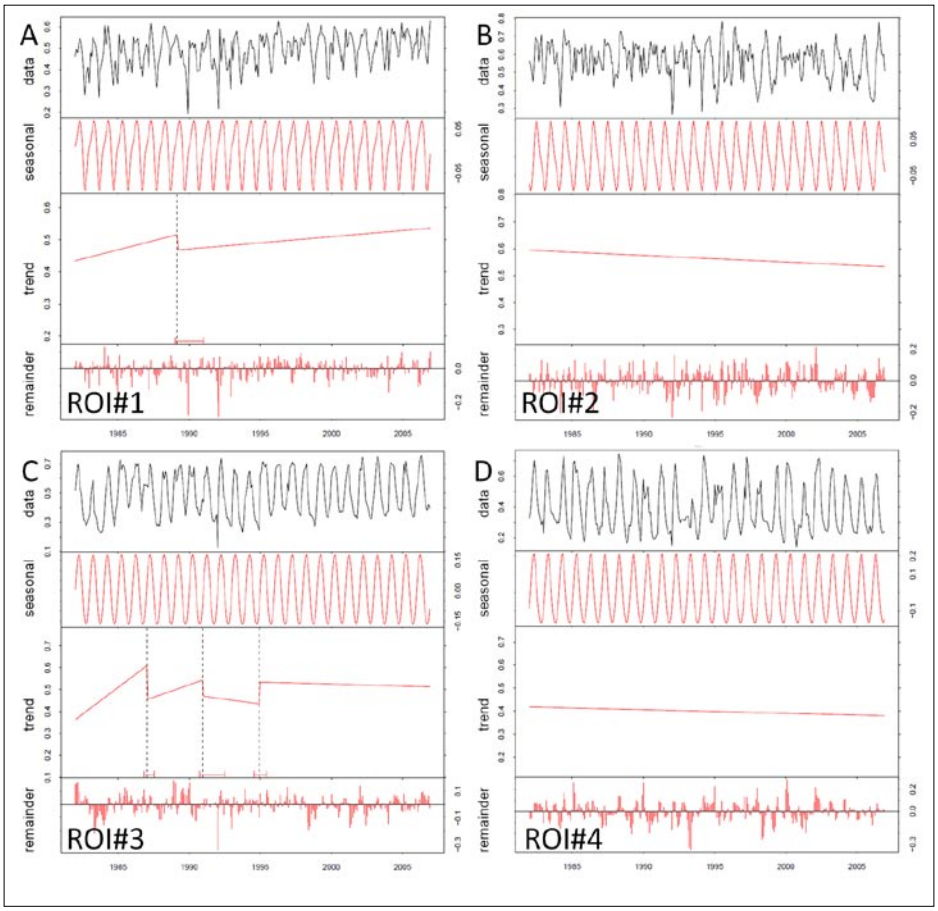

Figure 2 - Fitted seasonal, trend, and remainder components for monthly GIMMS NDVI time series (1982-2006) of certain ROIs, generated by BFAST approach. A) ROI #1, B), ROI #2, C) ROI #3, D) ROI #4.

All four regions show no breaks in the seasonal component. ROI #2 and ROI #4 present a continuous browning trend over the entire study period. ROI #1 shows a trend break at March 1989, separating two greening periods. ROI #3 is characterised by trend break at January 1987, December 1990, and December 1994, separating three greening and two

browning periods. The four examples already indicate a variety of different trends and trend breaks in NEB. Further analysis about the temporal occurrence of trend breaks in entire NEB need to be conducted to verify, if certain breakpoints occur over a larger area and are potentially caused by the same trigger.

Vegetation trends and their changes in NEB may relate to different triggers that could change from region to region. Erasmi et al. [2009] showed that vegetation greenness in NEB is strongly related to the seasonal precipitation cycle, which is also visible in the series of the ROIs (Fig. 3). Therefore, changes in precipitation amount and distribution may induce vegetation changes. Precipitation trends in NEB are sensitive to the duration and the beginning and end of the evaluated time period. Precipitation trends for the period 1982-2006 vary across NEB (Fig. 1D); yet no significant trend emerges for most of NEB.

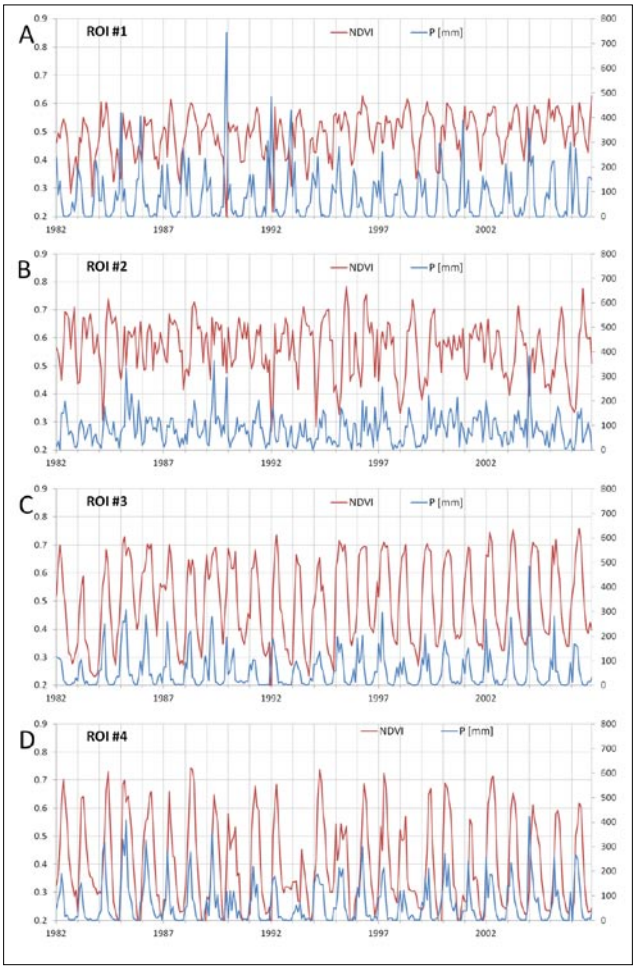

Figure 3 - Time series of monthly GIMMS NDVI (red) and GPCC precipitation (blue) data for the selected regions of interest. A) ROI #1; B) ROI #2; C) ROI #3; D) ROI #4.

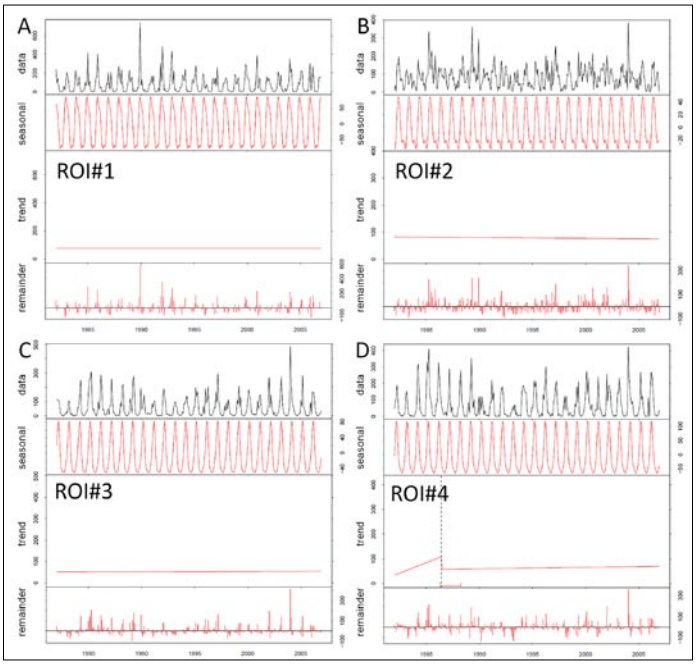

Figure 4 - Fitted seasonal, trend, and remainder components for monthly GPCC precipitation time series of certain ROIs generated by BFAST approach. A) ROI #1; B) ROI #2; C) ROI #3; D) ROI #4.

A larger adjacent area with significant negative precipitation trends is located in north-eastern Bahia and south-western Sergipe. One example for a larger area with a positive precipitation trend stretches from central Paraíba over central Pernambuco to northern Alagoas. The comparison of the trend component of NDVI (Fig. 2) and precipitation data (Fig. 4) for the selected ROIs, and the visual inspections of Figs. 1C and 1D show that the direction or absence of vegetation trends often do not match with the precipitation trend. For example, the pixels in the ROIs predominantly show a positive or negative NDVI long-term trend and mostly no long-term precipitation trend. While ROI #1 and ROI #3 show trend breaks in the NDVI data, just ROI #4 shows a trend break in the precipitation data. Although the comparison of NDVI and precipitation trends should be further expanded, these short considerations suggest that precipitation changes alone do not sufficiently explain the vegetation trends.

Land use changes and land degradation are important issues in the study area [Petta et al., 2005; MMA, 2007; Simielli, 2007; Costa Filho et al., 2008; da Costa et al., 2009; Boori and Amaro, 2010] and may lead to abrupt or gradual vegetation changes. However, the evaluation of land use changes and land degradation needs further information - especially ground truth data - than just coarse and moderate resolution NDVI data.

Strong El Niño-Southern Oscillation (ENSO) events probably also cause trend changes in the vegetation, as major droughts in NEB are related to El Niño phases [Rao, 1995; Hastenrath, 2006; Haylock et al., 2006]. Not all El Niño phases result in a drought in NEB, however [Kane, 1997; Erasmi et al., 2009]. Recently, Rodrigues et al. [2011] showed that

the inter-El Niño variability has to be taken into account, when accessing the effects of El Niño phases on precipitation in NEB. The authors highlighted that strong and long (weak and short) El Niño phases lead to dry (wet) conditions in NEB. The influence of El Nino variability on vegetation and trend changes should be analysed in future studies

Comparison of GIMMS and MODIS data set for 2001-2006

GIMMS and MODIS mean monthly NDVI and coefficients of variation show similar spatial patterns for NEB and are strongly linked with the major biomes of the study area (Fig. 5). MODIS data show predominantly higher mean NDVI values (Fig. 6B). Larger adjacent areas with differences (GIMMS - MODIS) of < -0.1 occur in north-western and south-eastern NEB.

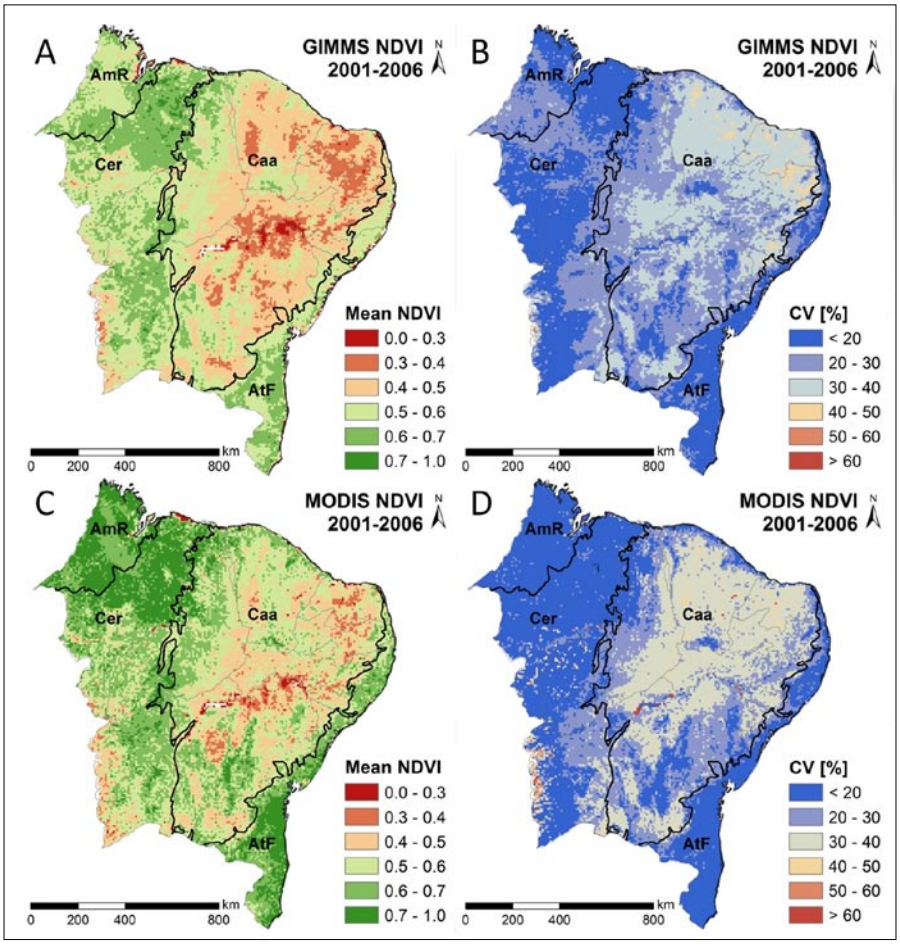

Figure 5 - Comparison of monthly NDVI values from GIMMS and MOD13A3 (resampled to 8 km resolution) for 2001-2006. A) Monthly mean of GIMMS; B) monthly CV of GIMMS; C) monthly mean of MODIS; D) monthly CV of MODIS. Black lines indicate biome borders after IBGE [2004a]: AmR = Amazon Rainforest; Cer = Cerrado; Caa = Caatinga; AtF = Atlantic Forest.

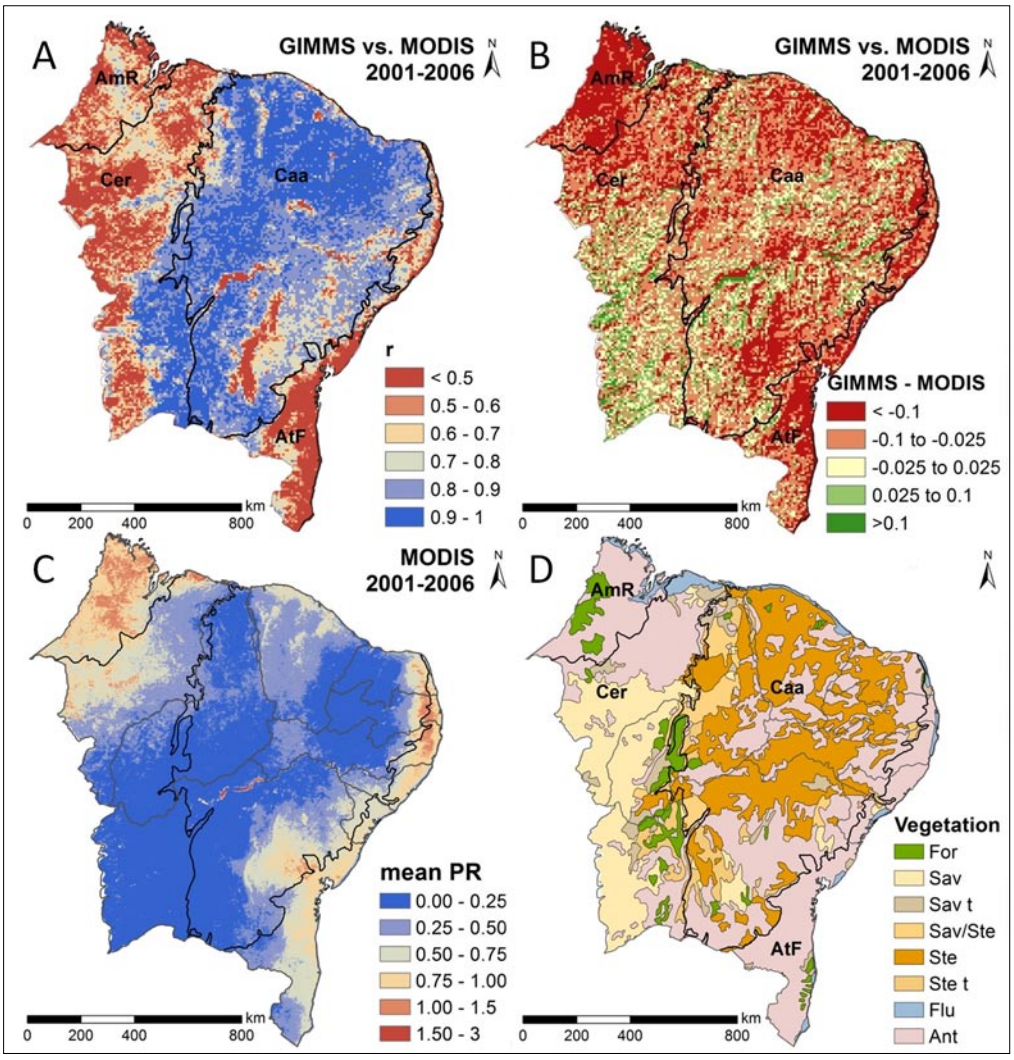

Figure 6 - Comparison of monthly NDVI values from GIMMS and MOD13A3 (re-sampled to 8 km spatial resolution) for 2001-2006. A) Correlation coefficient (*r*); B) difference of mean monthly NDVI: $GIMMS_{mean}$ - $MODIS_{mean}$; C) mean pixel reliability (PR) of monthly MODIS NDVI (0 = good data, 1 = marginal data, 2 = snow/ice, 3 = cloudy); D) Simplified vegetation types after IBGE [2004b]: For = forest, Sav = savanna, Sav t = savanna transition, Sav/Ste = savanna/steppe-like savanna, Ste = steppe-like savanna, Ste t = steppe-like savanna transition, Flu = fluviomarine/marine influenced vegetation, Ant = anthropogenically influenced regions (secondary vegetation or agriculture). Black lines indicate biome borders after IBGE [2004a]: AmR = Amazon Rainforest; Cer = Cerrado; Caa = Caatinga; AtF = Atlantic Forest.

The linear modelling between the GIMMS and the MODIS data sets results in a regional mean correlation coefficient of 0.71 for NEB, with strong intra-regional variability (Fig. 6A). Time series of both data sets for regions with different *r* values are exemplarily shown

for the four ROIs (Fig. 7). The highest correlation ($r \geq 0.8$) between GIMMS and MODIS NDVI can be found in the central part of NEB, whereas the lowest correlation ($r < 0.5$) is given along the eastern coast, the western part, and in isolated areas of central NEB (Fig. 6A). There are just a few pixels with negative *r* values that relate to water or partly wet areas and cities. The regional mean coefficient of determination for the entire study area is 0.56. The GIMMS data explains about 70 to 90% of the variance in the MODIS data in the high correlation areas in central NEB, and less than 50% in the low correlation areas.

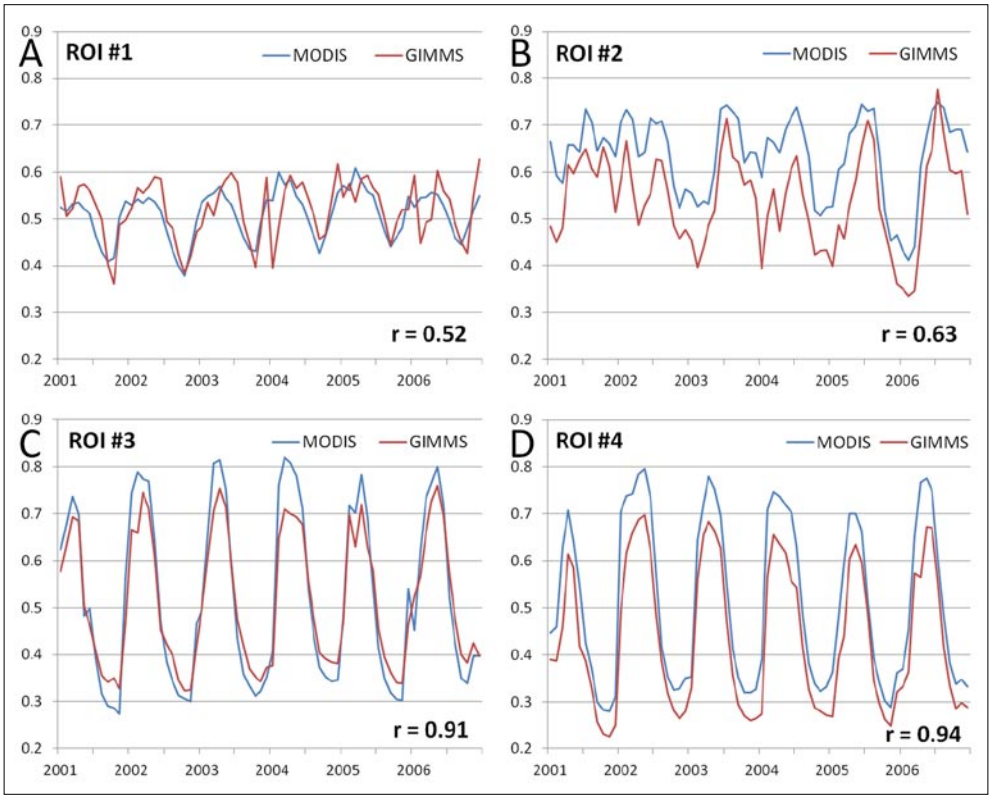

Figure 7 - Time series comparison of monthly NDVI data from GIMMS (red) and MODIS (blue) for the selected regions of interest. A) ROI #1; B) ROI #2; C) ROI #3; D) ROI #4; the corresponding correlation coefficient is displayed in the sub-figures.

The correlation between GIMMS and MODIS NDVI data seems to depend on vegetation properties like mean NDVI, CV, and hence vegetation type. In general, low *r* values relate to high mean NDVI values and vice versa. For example, low *r* value regions along the eastern coast represent the Atlantic Forest biome, low *r* value regions in the northwest correspond to the Amazon Rainforest and Cerrado biome; the larger isolated low *r* patch in central NEB represents the eastern part of the Diamantina plateau and mountains (Planaltos e Serras da Diamantina), and the high *r* value areas in central NEB roughly display the Caatinga biome. One larger exception from the described relationship between mean NDVI

and *r* value is found in south-western NEB. Here, the border between higher and lower *r* values does not mirror the border between the Caatinga and Cerrado biome. Instead, the lower *r* value regions represent the savanna vegetation type and the higher *r* values regions steppe-like savanna (typical for the Caatinga biome), seasonal deciduous forest, and transition vegetation (Fig. 6D). The pattern of the coefficient of variation of monthly NDVI values resembles the pattern of the correlation coefficient (partly even better than the mean NDVI): Regions with CV < 20% match approximately to regions with $r < 0.5$, and regions with higher CV (20-50%) show higher *r* values (≥ 0.8). Basically, the correlation between GIMMS and MODIS NDVI data is higher for vegetation with a high correlation coefficient and lower mean NDVI values.

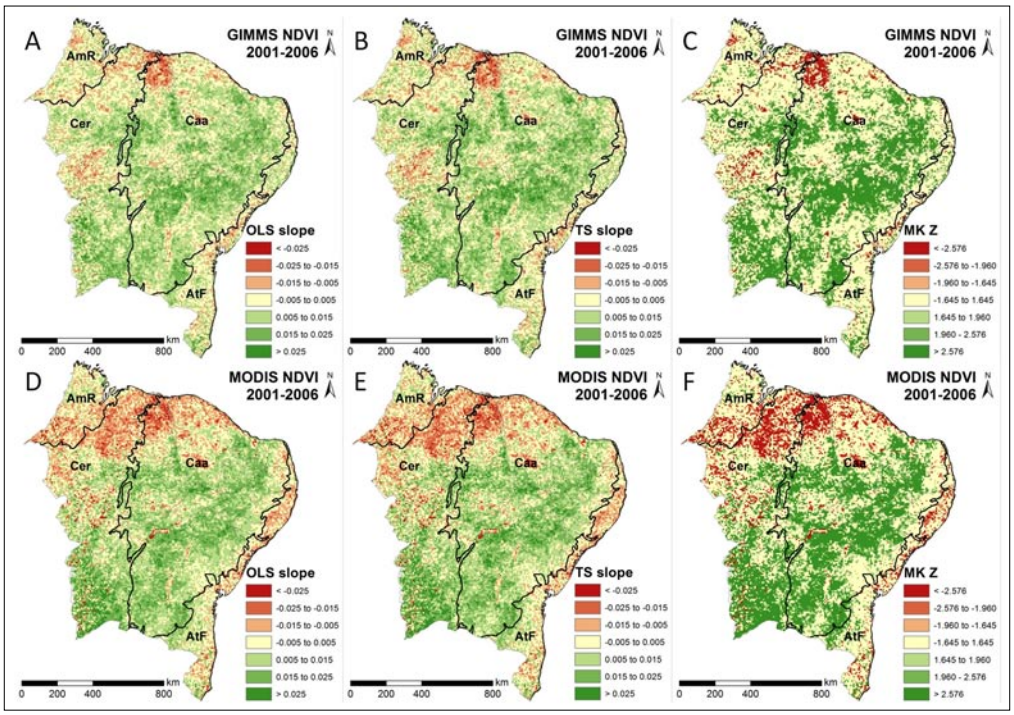

Figure 8 - Comparison of monthly NDVI values from GIMMS (top) and MOD13A3 (re-sampled to 8 km resolution; bottom) for 2001-2006. A+D) Slope of the linear trend calculated by ordinary least squares; B+E) slope of the Theil-Sen estimator; C+F) Mann-Kendall significance. Black lines indicate biome borders after IBGE [2004a]: AmR = Amazon Rainforest; Cer = Cerrado; Caa = Caatinga; AtF = Atlantic Forest.

According to the mean image of pixel reliability of the MODIS data (Fig. 6C), the best pixel reliability is found in the central part of NEB. The worst pixel reliability is associated with the areas along the east coast and in the northwest, which are characterised by the highest precipitation in NEB (Erasmi et al., 2009). The east-coast and northwest areas also represent regions with the lowest correlation coefficient. Therefore, one may assume that

cloud cover influences the compatibility of both data sets. But the patterns of pixel reliability (Fig. 6C) and correlation coefficient (Fig. 6A) in the southwest differ notably. While the pixel reliability is very good in the southwest, the correlation coefficient is two-part with low r values in the western part of the Cerrado and high values in the eastern part. We conclude that pixel reliability (mainly cloud cover) may have a certain influence on the compatibility of the data sets, but the more important factors are vegetation characteristics, as their pattern (especially CV) fit better to the pattern of the correlation coefficient.

All three trend estimators (OLS slope, TS slope, MK τ) show similar trend pattern for each NDVI data set (Fig. 8). The trends of the GIMMS and MODIS data set coincide rather well (mean difference of OLS slope of GIMMS - MODIS for entire NEB = 0.0014). Major differences are mainly related to north-western NEB, where the GIMMS data indicates predominantly no trend ($\alpha \geq 0.05$), and MODIS shows a negative trend. Another region with notably different trend behaviour is the coastal stripe, ranging from the state of Pernambuco via Alagoas to Sergipe. Both, the north-western and the eastern coast receive the highest mean precipitation sums in NEB. Similar results were found by Fensholt et al. [2009] for average annual trend analysis of GIMMS and MODIS data. They observed a good correspondence between the data sets for the semiarid Sahelian zone (200 to 1000 mm annual precipitation) and notable differences for regions with > 1000 mm annual precipitation.

In summary, the comparison between monthly NDVI values of the GIMMS and the MODIS data set reveal a varying compatibility of both data sets over NEB and partly confirm results of other studies like the predominantly higher NDVI values of the MODIS data [Fensholt and Sandholt, 2005; Brown et al., 2006]. Generally, the correlation between GIMMS and MODIS NDVI is higher for the lower NDVI regions, which are mainly attributed to the Caatinga biome. The trend analysis shows roughly similar pattern for both data sets.

Conclusions

The present study analysed GIMMS NDVI time series (1982-2006) to characterize long-term vegetation variability and trends in NEB. Monthly mean NDVI and monthly CV were used to assess the vegetation variability. Three trend estimators and the Mann-Kendall significance were calculated to evaluate temporal trends. Another aim of the study was the evaluation of the compatibility of GIMMS and MODIS NDVI data to support future data combination attempts. Therefore, both data sets were compared for the overlapping period 2001-2006 with respect to mean NDVI, CV, and trend behaviour.

Vegetation greenness is highly variable in space and time for NEB. Mean monthly NDVI and CV reflect the major biomes of NEB (and partly even vegetation types) with highest values in the Atlantic Forest biome along the Atlantic coast and in the Cerrado and Amazon Rainforest biome in western NEB. The central part of NEB, representing the Caatinga biome, shows the lowest mean NDVI values and the highest coefficient of variation. Besides the seasonal variability, NEB is characterized by a high inter-annual variability of vegetation greenness.

Long-term trend patterns of NDVI values vary notably within the study area. About 10% of the NEB area are affected by significant negative trends and about 28% by significant positive trends in the period 1982-2006. The overall trend pattern over entire NEB looks patchy with some larger adjacent areas of positive trend in the northwest and southwest, and some larger adjacent areas of negative trend in the central part and southeast of NEB. The analysis of ROIs indicate the occurrence of different browning and greening periods in NEB, which also

differ from place to place.

Future land degradation studies need to consider the high vegetation variability and trend changes in NEB. We recommend using time series instead of single pictures from some years to account for the natural vegetation variability in land degradation studies applying vegetation indices to evaluate vegetation changes. It is also important to verify the results obtained by NDVI data with ground truth data. Breaks in vegetation trends indicate abrupt vegetation changes and should be analysed in detail in future long-term studies.

The comparison between the GIMMS and MODIS NDVI values for the overlapping period reveal a strong variability across NEB. Generally, areas with a higher CV ($\geq 20\%$) and a lower mean NDVI (e.g., Caatinga) show a good correlation. For areas with a low CV ($<20\%$) and a higher mean NDVI (e.g., along the Atlantic coast and along the western border of NEB) the GIMMS NDVI data explain less than 50% of the variance of the MODIS NDVI data.

While the mean NDVI shows partly notable differences between both data sets, the trend analysis shows more or less similar patterns. For the GIMMS data, about 35% (5%) of NEB were affected by significant positive (negative) trends for the period 2001-2006, and for the MODIS, about 35% (13%) of the area were affected by positive (negative) trends. Larger trend differences between the two data sets occur in the northwest and along the east coast, whereby MODIS shows more negative trends.

Altogether, GIMMS and MODIS NDVI data seem to be more compatible for the dryer central part of NEB. Thereby, the trend pattern of both data sets match better than the mean NDVI. Future studies with the attempt to combine both data sets (e.g., for data continuity and up-scaling reasons) should try to increase the comparability between GIMMS and MODIS NDVI data - especially for regions with higher mean NDVI.

Acknowledgements

The first author thanks the Federal State of Saxony for the support by a PhD scholarship. We acknowledge the NASA Global Inventory Modeling and Mapping Studies (GIMMS) Group for producing and sharing the AVHRR GIMMS NDVI data set. NASA Land Processes Distributed Active Archive Center (LP DAAC) is thanked for sharing the MODIS vegetation indices product MOD13A3, which we obtained through the online Data Pool at the NASA (LP DAAC, USGS/Earth Resources Observation and Science (EROS) Center, Sioux Falls, South Dakota (http://lpdaac.usgs.gov/get_data). All authors are thankful to the responsible editor, Gherardo Chirici, and two anonymous referees for their thorough work and fine suggestions on an earlier version of this paper.

References

Almeida-Filho R., Carvalho C.M. (2010) - *Mapping land degradation in the Gilbues region, northeastern Brazil, using Landsat TM images.* International Journal of Remote Sensing, 31: 1087-1094. doi: http://dx.doi.org/10.1080/01431160903260957.

Barbosa H.A., Huete A.R., Baethgen W.E. (2006) - *A 20-year study of NDVI variability over the northeast region of Brazil*. Journal of Arid Environments, 67: 288-307. doi: http://dx.doi.org/10.1016/j.jaridenv.2006.02.022.

Boori M.S., Amaro V.E. (2010) - *Land use change detection for environmental management: using multi-temporal satellite data in the Apodi Valley of northeastern Brazil*. Applied

GIS, 6: 1-15.

Brown M.E., Pinzon J.E., Didan K., Morisette J.T., Tucker C.J. (2006) - *Evaluation of the consistency of long-term NDVI time series derived from AVHRR, SPOT-vegetation, SeaWiFS, MODIS, and Landsat ETM+ sensors*. IEEE Transactions on Geoscience and Remote Sensing, 44: 1787-1793. doi: http://dx.doi.org/10.1109/TGRS.2005.860205.

Chamaillé-Jammes S., Fritz H. (2009) - *Precipitation-NDVI relationships in eastern and southern African savannas vary along a precipitation gradient*. International Journal of Remote Sensing, 30: 3409-3422. doi: http://dx.doi.org/10.1080/01431160802562206.

Coppin P., Jonckheere I., Nackaerts K., Muys B., Lambin E. (2004) - *Digital change detection methods in ecosystem monitoring: a review*. International Journal of Remote Sensing, 25: 1565-1596. doi: http://dx.doi.org/10.1080/0143116031000101675.

Costa Filho A., Barbosa M.P., Petta A.R. (2008) - *O uso de geotecnologias no diagnóstico de risco a desertificação no Campo Petrolífero Canto do Amaro, município de Mossoró-RN*. Engenharia Ambiental, 5: 243-253.

da Costa T.C. e C., de Oliveira M.A.J., Accioly L.J. de O., da Silva F.H.B.B. (2009) - *Análise da degradação da caatinga no núcleo de desertificação do Seridó (RN/PB)*. Revista Brasileira de Engenharia Agrícola e Ambiental, 13: 961-974. doi: http://dx.doi.org/10.1590/S1415-43662009000700020.

CPRM (2009) - L*evantamento da geodiversidade, projeto atlas pluviométrico do Brasil, isoietas anuais médias período 1977 a 2006*. Serviço Geológico do Brasil.

Durpaire J.-P., Gentet T., Phulpin T., Arnaud M. (1995) - *SPOT-4 Vegetation instrument: Vegetation monitoring on a global scale*. Acta Astronautica, 35: 453-459. doi: http://dx.doi.org/10.1016/0094-5765(94)00279-U.

Eastman J.R. (2009) - *IDRISI Taiga - Guide to GIS and Image Processing*. Clark Labs, Worcester.

Erasmi S., Maurer F., Petta R.A., Gerold G., Barbosa M.P. (2009) - I*nter-annual variability of the Normalized Difference Vegetation Index over Northeast Brazil and its relation to rainfall and El Niño Southern Oscillation.* Geo-Öko, 30: 185-206.

Fensholt R., Rasmussen K., Nielsen T.T., Mbow C. (2009) - *Evaluation of earth observation based long term vegetation trends - Intercomparing NDVI time series trend analysis consistency of Sahel from AVHRR GIMMS, Terra MODIS and SPOT VGT data*. Remote Sensing of Environment, 113: 1886-1898. doi: http://dx.doi.org/10.1016/j.rse.2009.04.004.

Fensholt R., Sandholt I. (2005) - *Evaluation of MODIS and NOAA AVHRR vegetation indices with in situ measurements in a semi-arid environment*. International Journal of Remote Sensing, 26: 2561-2594. doi: http://dx.doi.org/10.1080/01431160600567761.

Gilbert R.O. (1987) - *Statistical methods for environmental pollution monitoring*. Van Nostrand Reinhold, New York.

Glenn E.P., Huete A.R., Nagler P.L., Nelson S.G. (2008) - *Relationship between remotely-sensed vegetation indices, canopy attributes and plant physiological processes: What vegetation indices can and cannot tell us about the landscape*. Sensors, 8: 2136-2160. doi: http://dx.doi.org/10.3390/s8042136.

Hastenrath S. (2006) - *Circulation and teleconnection mechanisms of Northeast Brazil droughts*. Progress in Oceanography, 70: 407-415. doi: http://dx.doi.org/10.1016/j.pocean.2005.07.004.

Haylock M.R., Peterson T.C., Alves L.M., Ambrizzi T., Anunciação Y.M.T., Baez J., Barros V.R., Berlato M.A., Bidegain M., Coronel G., Corradi V., Garcia V.J., Grimm A.M., Karoly D., Marengo J.A., Marino M.B., Moncunill D.F., Nechet D., Quintana J., Rebello E., Rusticucci M., Santos J.L., Trebejo I., Vincent L.A. (2006) - *Trends in total and extreme South American rainfall in 1960-2000 and links with sea surface temperature*. Journal of Climate, 19: 1490-1512. doi: http://dx.doi.org/10.1175/JCLI3695.1.

Huete A., Didan K., Miura T., Rodriguez X., Gao X., Ferreira L.G. (2002) - *Overview of the radiometric and biophysical performance of the MODIS vegetation indices*. Remote Sensing of Environment, 83: 195-213. doi: http://dx.doi.org/10.1016/S0034-4257(02)00096-2.

Huxman T.E., Smith M.D., Fay P.A., Knapp A.K., Shaw M.R., Loik M.E., Smith S.D., Tissue D.T., Zak J.C., Weltzin J.F., Pockman W.T., Sala O.E., Haddad B.M., Harte J., Koch G.W., Schwinning S., Small E.E., Williams D.G. (2004) - *Convergence across biomes to a common rain-use efficiency*. Nature, 429: 651-654. doi: http://dx.doi.org/10.1038/nature02561.

IBGE (2002) - *Mapa de clima do Brasil*. Instituto Brasileiro de Geografia e Estatística.

IBGE (2004a) - *Mapa de biomas do Brasil*. Instituto Brasileiro de Geografia e Estatística.

IBGE (2004b) - *Mapa de vegetação do Brasil*. Instituto Brasileiro de Geografia e Estatística.

de Jong R., Verbesselt J., Schaepman M.E., de Bruin S. (2012) - *Trend changes in global greening and browning: contribution of short-term trends to longer-term change*. Global Change Biology, 18: 642-655. doi: http://dx.doi.org/10.1111/j.1365-2486.2011.02578.x.

Justice C.O., Townshend J.R.G., Vermote E.F., Masuoka E., Wolfe R.E., Saleous N., Roy D.P., Morisette J.T. (2002) - *An overview of MODIS Land data processing and product status*. Remote Sensing of Environment, 83: 3-15. doi: http://dx.doi.org/10.1016/S0034-4257(02)00084-6.

Kane R.P. (1997) - *Prediction of droughts in north-east Brazil: Role of ENSO and use of periodicities*. International Journal of Climatology, 17: 655-665. doi: http://dx.doi.org/10.1002/(SICI)1097-0088(199705)17:6<655::AID-JOC144>3.0.CO;2-1.

Matschullat J., da Silva J., Höfle S., Mello J., Melo Jr G., Plessow A., Reimann C. (2012) - *A soil geochemical baseline for north-eastern Brazil*. Geochemistry: Exploration Environment Analysis, 12 (3): 197-209. doi: http://dx.doi.org/10.1144/1467-7873/10-RA-046.

MMA (2007) - *Atlas das areas susceptíveis à desertificação do Brasil*. Ministério do Meio Ambiente, Secretaria de Recursos Hídricos, Brasilia.

Morellato L.P.C., Haddad C.F.B. (2000) - *Introduction: The Brazilian Atlantic Forest*. Biotropica, 32: 786-792. doi: http://dx.doi.org/10.1111/j.1744-7429.2000.tb00618.x.

Myneni R.B., Hall F.G., Sellers P.J., Marshak A.L. (1995) - T*he interpretation of spectral vegetation indexes*. IEEE Transactions on Geoscience and Remote Sensing, 33: 481-486. doi: http://dx.doi.org/10.1109/36.377948.

NASA Land Processes Distribute Active Archive Center (2010) - *MOD13A3*. USGS/Earth Resources Observation and Science (EROS) Centre, Sioux Falls.

NASA Land Processes Distributed Active Archive Center (2012) - *MODIS Products Table*. Available at https://lpdaac.usgs.gov/products/modis_products_table (verified 22 June 2012).

Nimer E. (1989) - *Climatologia do Brasil*. IBGE, Departamento de Recursos Naturais e Estudos Ambientais, Rio de Janeiro.

Petta R., Ohara T., Medeiros C. (2005) - *Desertification studies in the Brazilian northeastern*

areas with GIS database. Anais XII Simpósio Brasileiro de Sensoriamento Remoto, INPE. Goiânia, pp.1053-1061.

Pinzon J.E., Brown M.E., Tucker C.J. (2005) - *EMD correction of orbital drift artifacts in satellite data stream.* In: Huang N.E., Shen S.S.P. (eds.) Hilbert-Huang transform and its applications. Interdisciplinary Mathematical Science. World Scientific Publishing Co. Pte. Ltd., Toh Tuck Link, pp. 167-186.

R Development Core Team (2012) - *R: A language and environment for statistical computing*. R Foundation for Statistical Computing, Vienna.

Rao V.B. (1995) - *On the severe drought of 1993 in north-east Brazil*. International Journal of Climatology, 15: 697-704. doi: http://dx.doi.org/10.1002/joc.3370150608.

Rodrigues R.R., Haarsma R.J., Campos E.J.D., Ambrizzi T. (2011) - *The impacts of inter-El Niño Variability on the tropical Atlantic and Northeast Brazil climate*. Journal of Climate, 24: 3402-3422. doi: http://dx.doi.org/10.1175/2011JCLI3983.1.

Rudolf B., Becker A., Schneider U., Meyer-Christoffer A., Ziese M. (2010) - *The new "GPCC Full Data Reanalysis Version 5" providing high-quality gridded monthly precipitation data for the global land-surface is public available since December 2010*. Global Precipitation Climatology Centre (GPCC), DWD, Internet Publication, pp. 1-7.

Rudolf B., Schneider U. (2005) - *Calculations of gridded precipitation data for the global land-surface using in-situ gauge observations*. Proceedings of the 2nd Workshop of the International Precipitation Working Group IPWG. Monterey, pp. 231-247.

Schneider U., Becker A., Meyer-Christoffer A., Ziese M., Rudolf B. (2011) - *Global Precipitation Analysis Products of the GPCC.* Global Precipitation Climatology Centre (GPCC), DWD, Internet Publication, pp. 1-12.

Simielli M.E. (2007) - *Geoatlas.* Editora Ática, São Paulo.

Tucker C.J., Pinzon J.E., Brown M.E. (2004) - *Global Inventory Modeling and Mapping Studies 2.0*. Global Land Cover Facility, University of Maryland, College Park.

Tucker C.J., Pinzon J.E., Brown M.E., Slayback D.A., Pak E.W., Mahoney R., Vermote E.F., El Saleous N. (2005) - *An extended AVHRR 8-km NDVI dataset compatible with MODIS and SPOT vegetation NDVI data.* International Journal of Remote Sensing, 26: 4485-4498. doi: http://dx.doi.org/10.1080/01431160500168686.

Tucker C.J., Yager K.A. (2011) - *Ten years of MODIS in space: lessons learned and future perspectives*. Italian Journal of Remote Sensing, 43: 7-18. doi: http://dx.doi.org/10.5721/ItJRS20114331.

UNCED (1992) - *Earth summit agenda 21: Programme of action for sustainable development*. United Nations Department of Public Information, New York.

Verbesselt J., Hyndman R., Newnham G., Culvenor D. (2010a) - *Detecting trend and seasonal changes in satellite image time series.* Remote Sensing of Environment, 114: 106-115. doi: http://dx.doi.org/10.1016/j.rse.2009.08.014.

Verbesselt J., Hyndman R., Zeileis A., Culvenor D. (2010b) - *Phenological change detection while accounting for abrupt and gradual trends in satellite image time series*. Remote Sensing of Environment, 114: 2970-2980. doi: http://dx.doi.org/10.1016/j.rse.2010.08.003.

Received 24/08/2012, accepted 03/10/2012